Full Paper

Fabrication and Properties of Conducting Polypyrrole/SWNT-PABS Composite Films and Nanotubes

Adam K. Wanekaya,[a,b] *Yu Lei*,[a,d] *Elena Bekyarova*,[b,c] *Wilfred Chen*,[a,b] *Robert Haddon*,[a,b,c] *Ashok Mulchandani*,*[a,b] *Nosang V. Myung**[a,b]

[a] Department of Chemical and Environmental Engineering, University of California, Riverside, California, 92521, USA
*e-mail: adani@engr.ucr.edu; myung@engr.ucr.edu
[b] Center for Nanoscale Science and Engineering, University of California, Riverside, California, 92521, USA
[c] Department of Chemistry, University of California, Riverside, California, 92521, USA
[d] Current Address: Division of Chemical and Biomolecular Engineering, Nanyang Technological University, Singapore 639798

Received: February 23, 2006
Accepted: April 4, 2006

Abstract
We report the electropolymerization and characterization of polypyrrole films doped with poly(m-aminobenzene sulfonic acid (PABS) functionalized single-walled nanotubes (SWNT) (PPy/SWNT-PABS). The negatively charged water-soluble SWNT-PABS served as anionic dopant during the electropolymerization to synthesize PPy/SWNT-PABS composite films. The synthetic, morphological and electrical properties of PPy/SWNT-PABS films and chloride doped polypyrrole (PPy/Cl) films were compared. Characterization was performed by cyclic voltammetry, atomic force microscopy (AFM), scanning electron microscopy (SEM) and Raman spectroscopy. SEM and AFM images revealed that the incorporation of SWNT-PABS significantly altered the morphology of the PPy. Cyclic voltammetry showed improved electrochemical properties of PPy/SWNT-PABS films as compared to PPy/Cl films. Raman Spectroscopy confirmed the presence of SWNT-PABS within composite films. Field effect transistor (FET) and electrical characterization studies show that the incorporation of the SWNT-PABS increased the electronic performance of PPy/SWNT-PABS films when compared to PPy/Cl films. Finally, we fabricated PPy/SWNT-PABS nanotubes which may lead to potential applications to sensors and other electronic devices.

Keywords: Polypyrrole, SWNT-PABS, Conducting Polymer, Composite Films, Nanotubes

DOI: 10.1002/elan.200603507

1. Introduction

Conducting polymers (CPs) contain π-electron backbone that is responsible for their unusual electronic properties such as controllable electrical conductivity, low energy optical transitions, low ionization potential and high electron affinity. The extended π-conjugated system of the conducting polymers has single and double bonds alternating along the polymer chains. These materials are particularly appealing because they exhibit electrical, magnetic, and optical properties of metals or semiconductors while retaining the attractive mechanical properties and processing advantages of polymers. Their conductivity can be reversibly modulated over 15 orders of magnitude by controlling the dopant type and level. Their unusual electronic and optical properties have made them very attractive materials in various applications including solar cells, light weight batteries, electrochromic devices, sensors and molecular electronic devices.

However, all known simple CPs are mechanically weak and have to be oxidized and doped by a counter anion to achieve significant conductivity. The strength of a conducting polymer may be improved by, for example, copolymerization with a second polymer such as poly(vinyl chloride) (PVC) but a sacrifice in conductivity is inevitable [1]. In addition, because dopants constitute a large proportion of conducting polymers, typically $20 \pm 40\%$ by volume, and all the dopants used so far are themselves insulators, the overall conductivity of CPs is somewhat limited [2].

On the other hand, carbon nanotubes (CNTs) have also provoked enormous interest in their fundamental behavior and a wide variety of potential applications. CNTs can be either metallic or semiconductive, depending on their helicity [3]. These one-dimensional fibers exhibit electrical conductivity as high as copper, thermal conductivity as good as diamond, strength 100 times greater than steel at one-sixth the weight, and have high strain to failure.

CNTs and CPs are both interesting for their unique electrochemical properties. In particular, composite materials based on the coupling of CPs and CNTs have been shown to possess properties of the individual components with a synergistic effect [4]. CNT-polymer composites were first prepared by Ajayan and co-worker by mechanically mixing multi-walled CNTs and epoxy resin [5]. Since then, many efforts have focused on the design and preparation of CNT-polymer composites, in order to obtain a new material that would possess properties that would be useful in particular applications [6, 7]. The CNT-doped PPy exhibits

dramatically different electronic properties compared to PPy prepared with small anionic dopants. Such differences reflect the conductivity of the CNT dopant compared to the common insulating dopants. The electron flow within the PPy/CNT composite is apparently increased by the entrapped CNTs due to an increased degree of delocalization and CNT bridging [6]. In fact, impedance studies indicated that PPy/CNT films are conducting even in their reduced state [6]. These characteristics have also been demonstrated in one-dimensional PPy/CNT nanostructures [8].

However, CNTs are difficult to process and insoluble in most solvents. In order to broaden their applications we found it necessary to tailor their solubility properties. We recently developed single-walled nanotubes (SWNTs) that were covalently functionalized with a water soluble conducting polymer, poly(m-aminobenzene sulfonic acid (SWNT-PABS) [9] (Fig. 1). The SWNT-PABS graft copolymer has excellent solubilities in water and some organic solvents and it also exhibits an order of magnitude increase in electrical conductivity over neat PABS. We also demonstrated that SWNT-PABS showed an improved sensor performance for the detection of NH_3 compared to unfunctionalized SWNTs because PABS is a conducting polymer in its own right [10]. Additionally, the SWNT-PABS sensors rapidly recover their resistance when NH_3 is replaced by nitrogen. The presence of numerous free amine groups in SWNT-PABS means that there is potential for covalent immobilization of various biomolecules. Further, its zwitterionic electronic structure and water solubility have been exploited in biological studies on the interactions of neurons with CNTs [11].

Based on the above we expect composite materials based on the coupling of CPs and SWNT-PABS to possess properties of each of the individual components with a synergistic effect. We hereby report the electropolymerization and characterization of polypyrrole composites doped with SWNT-PABS (PPy/SWNT-PABS). The negatively charged water-soluble SWNTs-PABS served as anionic dopant during electropolymerization. All prior works involving the polypyrrole and CNTs composites have been either done with multi-walled carbon nanotubes [7, 8] or carboxylic acid functionalized SWNTs [6, 8]. The SWNTs that we used were functionalized with PABS. PABS is a graft copolymer, therefore, the polypyrrole-SWNTs-PABS composites are well suited for biological research, sensor applications and other molecular electronic devices. We also extended our research to include field effect transistor studies and overoxidation of the conducting polymer-SWNT composites.

Characterization was performed by cyclic voltammetry, atomic force microscopy, Raman spectroscopy, scanning electron microscopy. Pyrrole was selected as our starting monomer because it is inexpensive, its polymerization is straightforward and well known, its electric and optical properties are reversibly controllable by both charge-transfer doping and protonation, it is environmentally stable and it can be electropolymerized at neutral pH which allows the entrapment of a wide range of biomolecules as demonstrated by us [12] and others [13, 14].

2. Experimental

2.1. Materials and Instrumentation

PABS functionalized SWNTs were provided by Carbon Solutions, Inc (www.carbonsolution.com, Riverside, CA). Pyrrole (98%) was purchased from Sigma-Aldrich (Milwaukee, WI) and was distilled prior to experiment. Porous alumina templates (Anodisc 13 with average pore size of 200 nm) were purchased from Whatman, Inc.). All solutions were prepared in nanopure water. Electrochemical and electrical characterization experiments were performed using VMP2 multichannel potentiostat/galvanostat (Princeton Applied Research, Princeton, NJ). The AFM images were recorded with a MultiMode Atomic Force Microscope Nanoscope3 (Veeco Instruments, Santa Barbara CA). The Raman spectra were recorded on a Bruker FT.

2.2. Synthesis of PPy/SWNT-PABS and PPy/Cl Films

The electrochemical deposition of PPy/SWNT-PABS films was carried out by cyclic voltammetry (between – 0.65 V to 1.05 V at 50 mV/s) or galvanostatically by applying a current density 3 mA/cm^2 for 6 minutes. The electropolymerization was conducted in a three-electrode cell with glassy carbon as the working electrode, Ag/AgCl as the reference electrode and platinum wire as the counter electrode. The electrolyte consisted of 0.25 M pyrrole monomer and 0.09 mg/mL SWNT-PABS in water. The negatively charged SWNT-PABS in solution acted as sole supporting electrolyte and dopant for the PPy deposition. The resulting films were washed with nanopure water before analysis. For comparison, PPy/Cl films were prepared under the same conditions using aqueous solution of 0.5 M NaCl instead of SWNT-PABS. The films were characterized by cyclic voltammetry in aqueous 0.5 M NaCl solution at a scan rate of 50 mV/s.

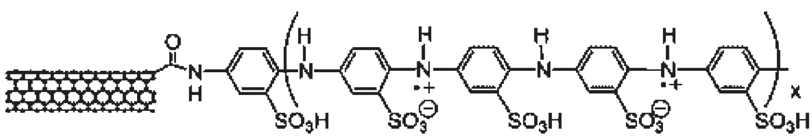

Fig. 1. Chemical structure of SWNTs functionalized with PABS.

2.3. Electrodeposition Between Microfabricated Electrodes

For electrical characterization and field effect transistor (FET) studies, the electrodes were microfabricated on a (100)-oriented silicon wafer with a chemical vapor deposition (CVD) grown 1 μm thick insulator layer of low-stress Si_3N_4 film. A Cr adhesion layer and ~3000 Å Au layer were then deposited. The distance between the two gold electrodes was 3 μm.

A 2 μL drop of the electrolyte solution containing 0.25 M pyrrole and 0.09 mg/mL SWNT-PABS in water was introduced between the gold electrodes, and the electrodeposition of the PPy/SWNT-PABS film took place from the anode to the cathode under applied current of 1 mA. The growth of the film was monitored using a chronopotentiogram and terminated as the potential value dropped to ~0 V. PPy/Cl film was similarly grown in aqueous 0.5 M NaCl.

2.3.1. Electrical Characterization of Composite Films

The $I-V$ characteristic of the composite films was performed by introducing 2 μL of 0.1 M aqueous NaCl on the films between the gold electrodes followed by a linear sweep of the voltage between -0.1 V and $+0.1$ V at 50 mV/s. Breakdown voltage measurements were performed on the dry films at ambient conditions. The voltage between the gold electrodes separated by the film was swept from 0 V to 10 V at 200 mV/s.

The PPy films were configured into a liquid ion gated field effect transistor by converting the reference Ag/AgCl into a "liquid ion gate electrode" while the two gold electrodes represented the "source" and "drain electrode". The gate potential was varied from -0.6 V to 3.0 V while monitoring the drain current and the drain voltage.

2.4. Synthesis of PPy/SWNT-PABS Nanotubes

PPy/SWNT-PABS and PPy/Cl nanotubes were fabricated using template-directed electrochemical deposition. Before the synthesis of the PPy/SWNT-PABS nanotubes, Platinum metallic seed layers (approximately 500 nm thick) were sputtered using Emitech K550 table-top sputter. The template was fixed to a glass support with the seed layer face down using double-sided conductive copper tape. Single-sided conductive copper tape was used as a lead to the glass support. The entire sample, except for the middle of the template and the end of the copper tape lead, was masked with a commercially available dielectric material. (Microstop, Pyramid Plastics, Inc.).

The PPy/SWNT-PABS nanotubes were deposited through the template pores in an aqueous solution of 0.25 M pyrrole monomer and 0.09 mg/mL SWNT-PABS dopant. The electrolyte solution was deaerated with 99.999% nitrogen prior to the electropolymerization process. The electropolymerization was conducted in a three-electrode electrochemical cell with sputter coated alumina template as working electrode. Ag/AgCl and a platinum coated titanium plate were used as reference electrode and auxiliary electrode, respectively. The PPy/SWNT-PABS nanotubes were deposited by galvanostatically at 3 mA cm^{-2}. After deposition, the alumina template working electrode was rinsed thoroughly with water and soaked in 1 M aqueous NaOH for 6 hours in order to selectively dissolve the alumina template. After rising with water, the free-standing PPy/SWNT-PABS nanotubes were produced.

3. Results and Discussion

Figure 2 shows the cyclic voltammetry (CV) growth of PPy/SWNT-PABS and PPy/Cl films on a gold electrode. Since the SWNT-PABS were the only species in solution other than pyrrole in the formation of PPy/SWNT-PABS film, this implied that the SWNT-PABS acted both as electrolyte and dopant as indicated by an increase in current with electrolysis time and by the formation of a black coating. Furthermore, an increase in SWNT-PABS concentration in the electrolyte medium accelerated the growth of the polymer coating, demonstrating that SWNT-PABS indeed participated in the electrochemical polymerization. No coating was observed during electrochemical polymerization of SWNT-PABS in the absence of pyrrole. This is additional evidence that SWNT-PABS acted as a dopant in the electropolymerization process. A comparison of the CVs of the PPy/SWNT-PABS and PPy/Cl film formation reveals that the currents attained in the case of PPy/Cl are much higher due the much easier entrapment of the smaller Cl^- anion compared to the much more bulkier SWNT-PABS species.

Figure 3 shows the cyclic voltammogram (CV) characterization of the PPy/Cl and PPy/SWNT-PABS films in 0.5 M NaCl. There are fundamental differences in the two CVs. First, the output current of the PPy/SWNT-PABS film is five times that of the PPy/Cl film. This implies that the capacitance of the former is about five times that of the latter film. This phenomenon has also been observed by other workers [15, 16]. Secondly, the peak potential of the PPy/SWNT-PABS film is about 200 mV more negative than that of PPy/Cl film confirming the anionic dopant role of SWNT-PABS [6]. The third difference is that the PPy/SWNT-PABS film is electrochemically active in much a wider potential window than PPy/Cl film. The window in which PPy/SWNT-PABS is active ranges from -0.6 V compared to -0.4 V for PPy/Cl indicating that the presence of SWNTs in PPy promotes the electron transfer of the redox processes and lessens the electrokinetic polarization [6]. The above observations indicate that PPy/SWNT-PABS has obviously different electronic properties compared to PPy/Cl films or other PPy films containing small anionic and insulating dopants. The above results demonstrate two points, first, SWNT-PABS works as the anionic dopant in PPy instead of a simple nanofiller, [6] second, the sharp peak and the peak potential shift is attributed to the unique properties of doped SWNT-PABS. The peak potential

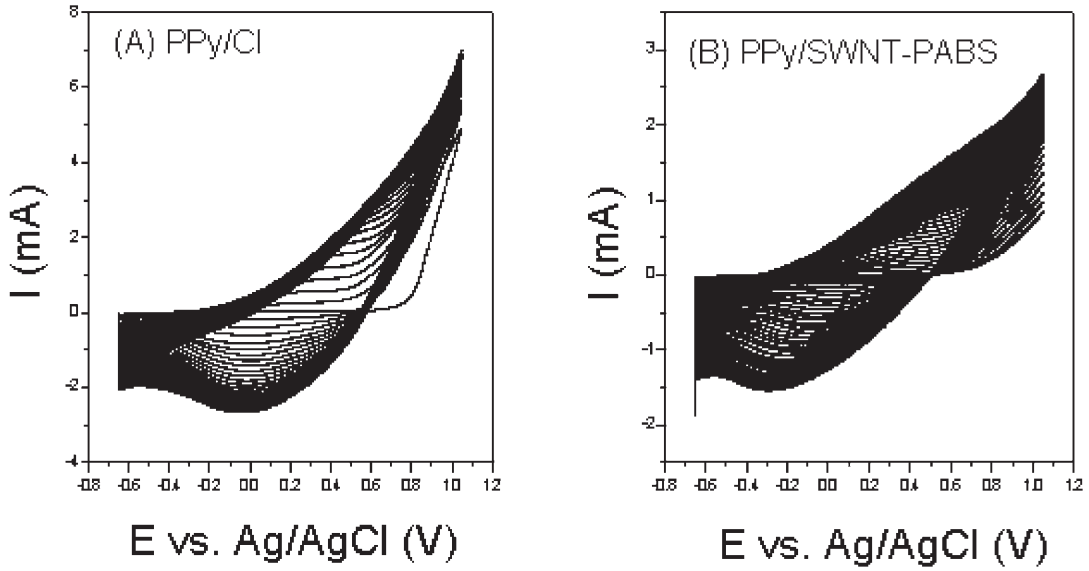

Fig. 2. Cyclic voltammograms of the film growth of PPy/SWNT-PABS and PPy/Cl. Electrolyte: 0.25 M aqueous pyrrole containing 0.09 mg/mL SWNT-PABS. Scan rate: 50 mV/s, 50 cycles.

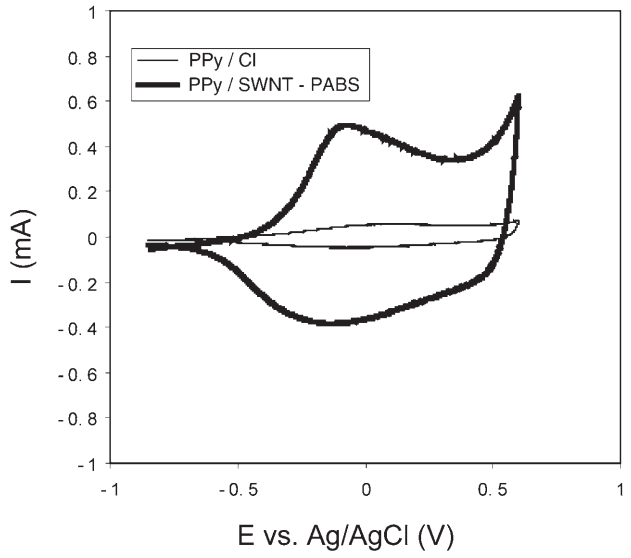

Fig. 3. Cyclic voltammograms for the comparison of PPy/SWNT-PABS composite film and PPy/Cl^- film prepared under same conditions. Scan rate 50 mV/s, electrolyte 0.5 M NaCl.

located in the negative range also makes the composite film an ideal material in sensor application.

The surface morphology of the films was characterized by scanning electron microscopy (SEM) and atomic force microscopy (AFM). As shown in Figure 4, the surface morphology of PPy/SWNT-PABS film was significantly different from that of PPy/Cl film. The surface of PPy/Cl films shows typical granular morphology and it is appears less smooth compared to the PPy/SWNT-PABS film which exhibits fibrillar morphology. The granules in PPy/Cl film range from 1 micron to almost 3 microns. The PPy coating on the SWNT-PABS is very evident and this results into polymer coating of 150 nm in thickness. The diameter of the PPy/SWNT-PABS fibrils is significantly larger than that of the SWNT-PABS alone. This is indicative of good interaction between the SWNT-PABS dopants and pyrrole monomer because the SWNT-PABS acted both as a dopant and also provided a large surface area for the polymerization process to take place. The randomly oriented fibrils were consistently coated with polymer films. This porous morphology allows for excellent electrolyte access with less resistance. The high conductivity of SWNT doped in the composite film increases the electrical properties of the redox processes and also provides a large surface area available for PPy intercalation. Figure 5 shows AFM images of PPy/Cl and PPy/SWNT-PABS. The different morphologies in the two films observed in SEM were also observed by AFM. For example, the surface of PPy/Cl shows typical granular morphology and it is appears less smooth compared to the PPy/SWNT-PABS film which exhibits fibrillar morphology.

The current – voltage ($I-V$) characteristics of PPy/Cl and PPy/SWNT-PABS films are significantly different (Fig. 6). The $I-V$ curve of PPy/Cl has the characteristic "S" shape that depicts its semiconducting character [17, 18]. On the other hand, the $I-V$ curve of PPy/SWNT-PABS follows Ohm's low reflecting its metallic character due to enhancement of electron flow by the entrapped SWNT-PABS which may also serve as conducting bridges between different PPy domains.

Figure 7 shows the plot of resistance vs. the gate potential (V_G) of PPy/Cl and PPy/SWNT-PABS composite films in 0.1 M NaCl solution using liquid ion gated field effect transistor configuration. In general, there is a decrease in the resistance of the film as V_G is changed from negative to positive potentials reaching a minimum at about 1.6 V. The decrease in the resistance of the films as V_G is scanned as

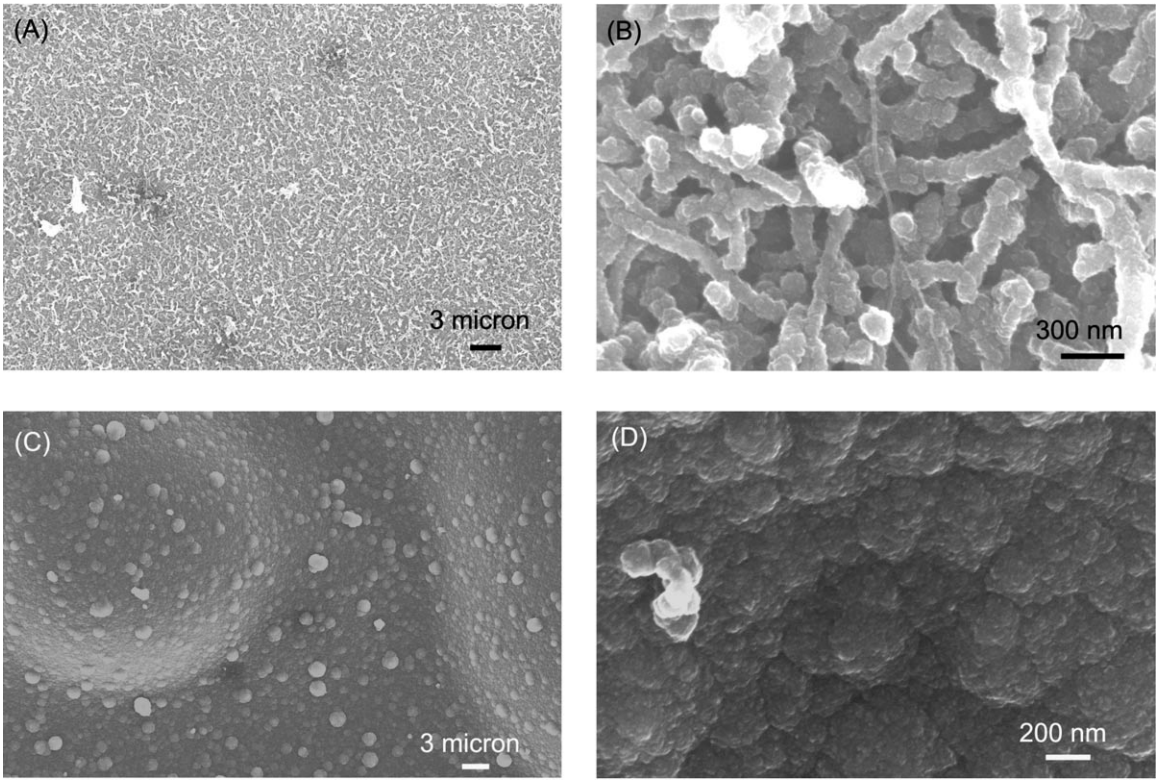

Fig. 4. SEM images PPy/SWNT-PABS film (A and B) and PPy/Cl film (C and D).

described above is consistent with what other workers have with PPy films [19] and other pyrrole derivative-based polymer films [20]. After 1.6 V there is a sharp increase in resistance of PPy/Cl film from about 2 kΩ to about 10 MΩ which is almost four orders of magnitude. The sudden increase in resistance suggests that the PPy/Cl film was degraded resulting in the massive loss conducting capability within the polymer matrix. The resistance of the PPy/Cl film leveled off after potentials of more than 1.6 V. The degradation is induced by anodic polarization and is described in the literature as overoxidation.

On the other hand, the resistance values in the case of the PPy/SWNT-PABS film were more or less constant till after potentials of more than 2.5 V. A gradual increase of resistance with increase of potentials to more positive values was observed. These observations are consistent with the overoxidation process of the polymer. Unlike the PPy/Cl film, the PPy/SWNT-PABS film is overoxidized at more positive potentials than 1.6 V and this could be due to the possibility that the presence of the SWNT-PABS discourages the anodic polarization process which resulted in the degradation and overoxidation of the PPy/Cl to occur much sooner. This observation implies that PPy/SWNT-PABS can be utilized at much more positive potentials than PPy/Cl.

It has been suggested that overoxidation interrupts conjugation by formation of hydroxyl and carbonyl species and, eventual loss of material through formation of CO_2. These electrical and chemical changes have indeed been detected by subtractively normalized interfacial Fourier transform infrared spectroscopy [21] and infrared reflective absorption spectroscopy [22].

It can also be observed from Figure 7 that the change in resistance with the variation in V_G is much larger in the case of PPy/Cl than PPy/SWNT-PABS. The resistance change is about 10^3 Ω between 0.3 V and 1.5 V for PPy/Cl. This phenomenon is well known and documented as the resistance of conducting polymers depend on their electrochemical potential [23]. In fact changes in resistance of $> 10^6$ have been routinely found by this procedure [23]. On the other hand, the change in resistance for PPy/SWNT-PABS is just one order of magnitude in the same potential window because the SWNT-PABS dopant is conducting. Therefore, variation of V_G would not change the resistance as much as it would in the case of PPy/Cl which has an insulating dopant.

The breakdown voltage (V_b) of the PPy films was determined by sweeping the potential between the two gold electrodes from 0 V to 10 V at 200 mV/s in air at ambient conditions (Fig. 8). The current increased with increase in potential until it reached maximum followed by a plateau phase and finally a gradual decrease. The PPy/Cl film attained maximum current at about 1.7 V. The plateau phase extended up to 2.5 V. Based on these observations it is evident that there is some form of degradation of the electrical properties of the PPy/Cl film after 1.7 V. Degradation of electrical properties means a gradual decrease in conductivity and this is the breakdown voltage of the PPy/Cl film which is approximately 1.7 V. On the other hand, the V_b

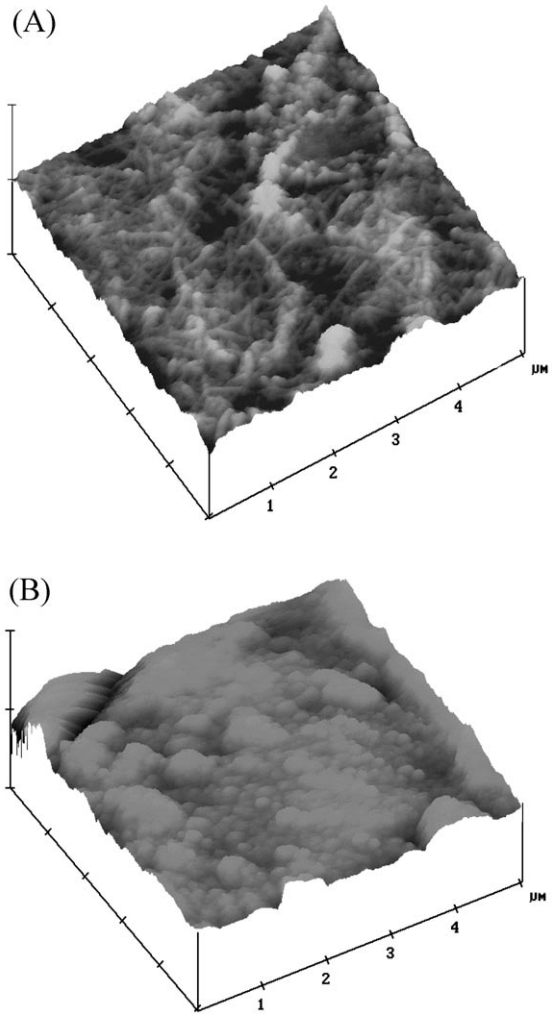

Fig. 5. AFM images of PPy/SWNT-PABS (A) and PPy/Cl (B).

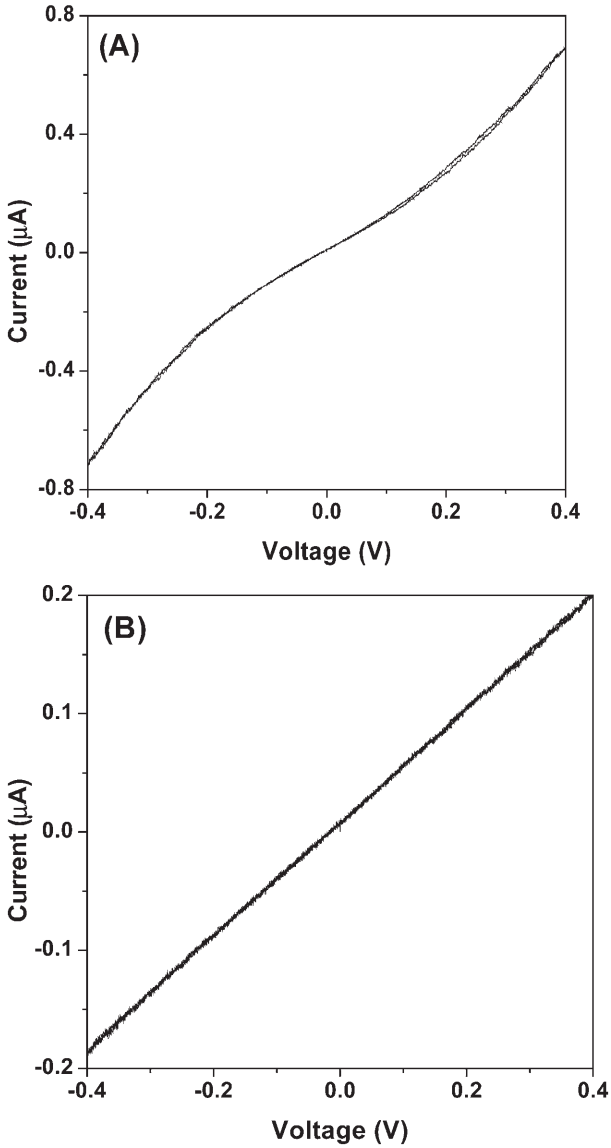

Fig. 6. $I-V$ characteristics of PPy/Cl (A) and PPy/SWNT-PABS (B) films. Electrolyte = 0.1 M NaCl, scan rate = 50 mV/s.

of the PPy/SWNT-PABS is about 8.5 V since this is the potential at which the current is maximum. Since this process occurred in the dry state, the probable oxidizing agent that initiated the overoxidation of PPy is oxygen in the atmosphere to generate carbonyls or CO_2 [24]. As mentioned earlier, the presence of the SWNT-PABS increases the electrical strength of the film by serving as "conducting bridges" connecting the conducting domains of PPy.

Figure 9 shows the SEM images of the PPy/SWNT-PABS nanotubes synthesized within the 200 nm diameter alumina pores. The nanotubes are fairly uniform in size and morphology with the expected diameter of approximately 200 nm from template pores. It is also evident that the PPy/SWNT-PABS nanotubes are hollow, partially due to surface soaking phenomena in pores during template-direct electropolymerization. More interestingly, some undoped SWNT-PABS were even visible in high-magnification SEM images as indicated in Figure 9. The easy fabrication of size-controllable PPy/SWNT-PABS nanotubes shows great promise for nanodevice applications.

The structure of the synthesized PPy/SWNT-PABS nanotubes was also characterized using Raman spectroscopy (Fig. 10). The spectra of the conducting PPy/SWNT-PABS show the two most prominent features typically observed in the Raman spectra of SWNTs and associated with the radial breathing mode (175 cm^{-1}) and tangential mode (G-band at 1596 cm^{-1}) of the carbon atoms on the SWNT walls [25, 26]. The same peaks are observed in the spectra of SWNT-PABS. The Raman scattering from pure PPy/Cl gives a peak in the range of the G-band associated with sp^2-hybridized carbon atoms, however the peak is broad and of very low intensity (Fig. 10). Importantly, the D-band with a maximum at 1296 cm^{-1} arising from disordered sp^3-hybridized carbon present as impurities and defects in SWNTs has similar intensity in both SWNT-PABS and PPy/SWNT-PABS, which indicates that the electronic structure of the SWNT-PABS is not perturbed as a result of being incorporated into PPy.

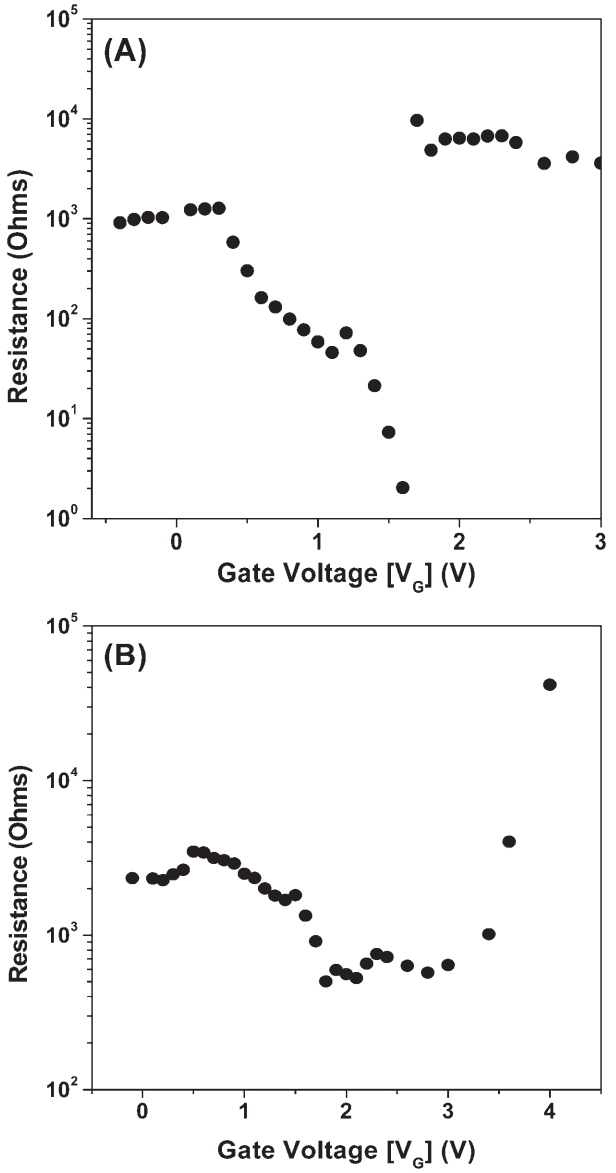

Fig. 7. A) Resistance vs. gate voltage of PPy/Cl film in 0.1 M aqueous NaCl. B) Resistance vs. gate voltage of PPy/SWNT-PABS film in 0.1 M aqueous NaCl.

4. Conclusion

We reported the synthesis and properties of composite material PPy/SWNT-PABS film/nanotube using water-soluble single-walled carbon nanotube-poly(m-aminobenzene sulfonic acid) copolymer (SWNT-PABS). The water-soluble SWNT-PABS were homogeneously dispersed in the pyrrole solution and acted both as a supporting electrolyte and a dopant in the electropolymerization process. SEM and AFM results indicated that the doped SWNT-PABS significantly changed the morphology of PPy and the composite film formed porous and crossed network. Field effect transistor (FET), $I-V$ characteristics, and V_b studies confirmed that the incorporation of the SWNT-PABS increased the electronic performance of PPy/SWNT-PABS film when

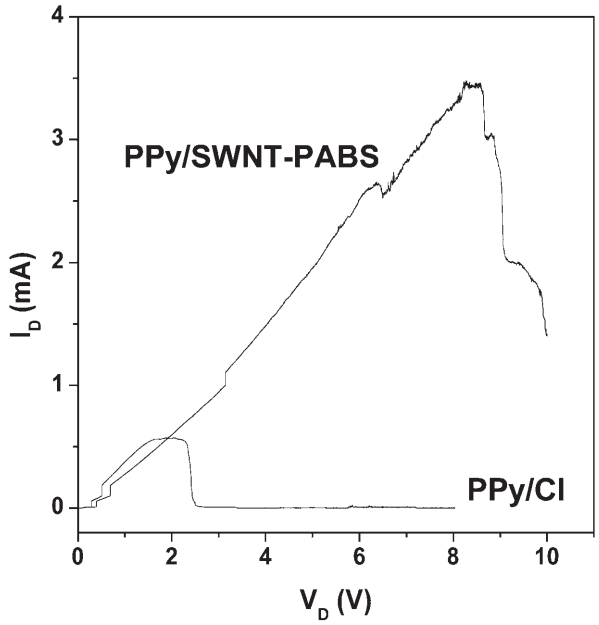

Fig. 8. Breakdown voltage of PPy/Cl and PPy/SWNT-PABS films in air. Scan rate = 200 mV/s.

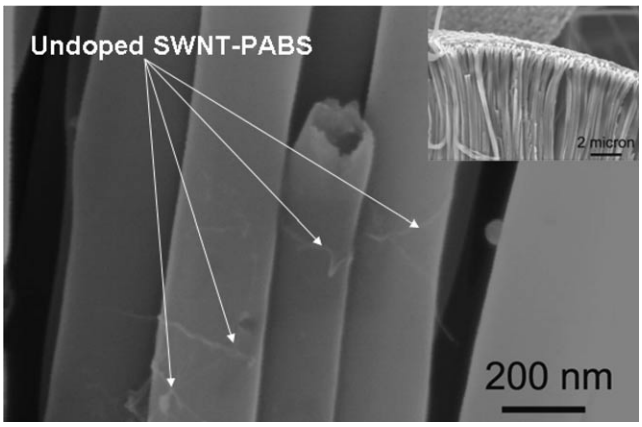

Fig. 9. SEM images of PPy/SWNT-PABS nanotubes. Inset: A low resolution SEM image of bundle of nanotubes.

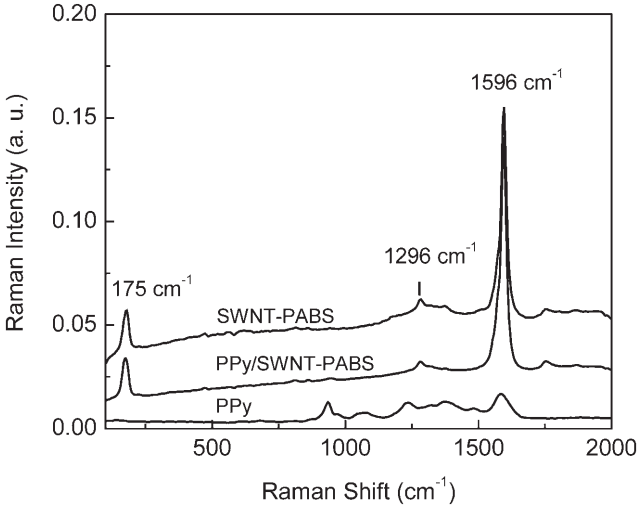

Fig. 10. Raman spectra of PPy, PPy/SWNT-PABS, and SWNT-PABS nanotubes.

compared to PPy film. Finally, PPy/SWNT-PABS nanotubes were synthesized and these new one-dimensional conducting polymer-SWNT-PABS nanotube composite materials are well suited for biological research, sensor applications and other molecular electronic devices as a result of the enhanced electron flow and grafted nature

5. Acknowledgement

We acknowledge the support of this work by grants H94003-04-2-0404 from DOD/DARPA/DMEA, BES-0529330 from the NSF, and GR-83237501 from the U.S. EPA.

6. References

[1] A. M. Waller, A. N. S. Hampton, R. G. Compton, *J. Chem. Soc., Faraday Trans.* **1989**, *85*, 773.
[2] B. R. Saunders, R. J. Fleming, K. S. Murray, *Chem. Mater.* **1995**, *7*, 1082.
[3] T. W. Odom; J.-L. Huang, P. Kim, C. M. Lieber, *Nature* **1998**, *391*, 62.
[4] M. Hughes, G. Z. Chen, M. S. Shaffer, D. J. Fray, A. H. Windle, *Chem. Mater.* **2002**, *14*, 1640.
[5] P. M. Ajayan, O. Stephan, C. Colliex, D. Trauth, *Science* **1994**, *256*, 1212.
[6] G. Z. Chen, M. S. P.Shaffer, D. Coleby, G. Dixon,; W. Zhou, D. J. Fray, A. H. Windle, *Adv. Mater.* **2000**, *12*, 522.
[7] G. Han, J. Yuan, G. Shi, F. Wei, *Thin Solid Films* **2005**, *474*, 64.
[8] J. Wang, J. Dai, T. Yarlagadda, *Langmuir* **2005**, *21*, 9.
[9] B. Zhao, H. Hu, R. C. Haddon, *Adv. Funct. Mater.* **2004**, *14*, 71.
[10] E. Bekyarova, M. Davis, T. Burch, M. E. Itkis, B. Zhao, S. Sunshine, R. C. Haddon, *J. Phys. Chem. B* **2004**, *108*, 19717.
[11] H. Hu, Y. Ni, V. Montana, R. C. Haddon, V. Parpura, *Nano Lett*. **2004**, *4*, 507.
[12] K. Ramanathan, M. A. Bangar, M. Yun, W. Chen, N. V. Myung, A. Mulchandani, *J. Am. Chem. Soc.* **2005**, *127*, 496.
[13] S. Cosnier, *Anal. Bioanal. Chem*. **2003**, *377*, 507.
[14] J.-C. Vidal, E. Garcia-Ruiz, J.-R. Castillo, *Microchim. Acta* **2003**, *143*, 93.
[15] C. Y. Liu, A. J. Bard, F. Wudl, I. Weitz, J. R. Heath, *Electrochem. Solid State Lett*. **1999**, *2*, 577.
[16] C. Downs, J. Nugent, P. M. Ajayan, D. J. Duquette, S. V. Sanatham, *Adv. Mater.* **1999**, *11*, 1028.
[17] H. J. Lee, S.-M. Park, *J. Phys. Chem. B* **2004**, *108*, 1590.
[18] S. K. Saha, Y. K. Su, C. L. Lin, D. W. Jaw, *Nanotechnology* **2004**, *15*, 66.
[19] G. P. Kittlesen, H. S. White, M. S. Wrighton, *J. Am. Chem. Soc*. **1984**, *106*, 7389.
[20] D. Ofer, R. M. Crooks, M. S. Wrighton, *J. Am. Chem. Soc*., **1990**, *112*, 7869.
[21] P. Novak, B.Rasch, W. Vielstich, *J. Electrochem. Soc.* **1991**, *138*, 3300.
[22] F. Beck, P. Braun, M. Oberst, *Ber. Busenges. Phys. Chem*. **1987**, *91*, 967.
[23] E. W. Paul, A. J. Ricco, M. S. Wrighton, *J. Phys. Chem.* **1985**, *89*, 1441.
[24] W. M. Wang, H. H. Wan, T. W. Rong, J. R. Bao, S. H. Lin, *Nuclear Instruments and Methods in Physics Research B61* **1991**, 466.
[25] A. M. Rao, E. Richter, S. Bandow, B. Chase, P. C. Eklund, K. A. Williams, S. Fang, K. R. Subbaswamy, M. Menon, A. Thess, R. E. Smalley, G. Dresselhaus, M. Dresselhaus, *Science* **1997**, *275*, 187.
[26] M. S. Dresselhaus, G. Dresselhaus, A. Jorio, A. G. Souza Filsho, M. A. Pimenta, R. Saito, *Acc. Chem. Res.* **2002**, *35*, 1070.

